DOI:
10.1109/EMBC.2015.7319642

Document Version
Peer reviewed version

Disposable Soft 3 Axis Force Sensor for Biomedical Applications

Damith Suresh Chathuranga[1], Zhongkui Wang[1], Yohan Noh[2], Thrishantha Nanayakkara[2] and Shinichi Hirai[1]

***Abstract*— This paper proposes a new disposable soft 3D force sensor that can be used to calculate either force or displacement and vibrations. It uses three Hall Effect sensors orthogonally placed around a cylindrical beam made of silicon rubber. A niobium permanent magnet is inside the silicon. When a force is applied to the end of the cylinder, it is compressed and bent to the opposite side of the force displacing the magnet. This displacement causes change in the magnetic flux around the ratiomatric linear sensors (Hall Effect sensors). By analysing these changes, we calculate the force or displacement in three directions using a lookup table. This sensor can be used in minimal invasive surgery and haptic feedback applications. The cheap construction, bio-compatibility and ease of miniaturization are few advantages of this sensor. The sensor design, and its characterization are presented in this work.**

I. INTRODUCTION

Most autonomous systems used in biomedical applications require force and displacement measurements. For example, in minimal invasive surgery (MIS) a surgeon would benefit much if laparoscope had a sensor to measure the stiffness of organ tissue. Then, a physician would touch organ tissue with the probe and asses its stiffness similar to a finger palpation to find abnormalities in stiffness. This feedback would greatly increase the detection of cancer and other potential illnesses. Furthermore, force sensors in teleoperated robot hands would give tactile feedback to the physician on the other side of the device while examining abdomen conditions of the patient to detect signs of abdominal guarding. Moreover, automated probes may have higher chance of identifying stiffness variations than surgeons because the robotic tactile systems can be precise than human mechanoreceptors, as sensory adaptation is absent. Though, there are many proposed force measurement devices for general purpose measurements, very few can be used in biomedical applications. This is because if these to be used in biological applications, it has to be either disposed or sanitized after use according to the best medical practices. Therefore, the sensor needs to be cheap if it to be disposed or if it to be reused, should be able to withstand temperatures above 121 °C, and pressures above 103 kPa for a period of 15 minutes.

This research was supported in part by JSPS Grant-in-Aid for Scientific Research 15H02230.

[1]Damith Suresh Chathuranga, Zhongkui Wang and Shinichi Hirai are with the Department of Robotics, Graduate School of Science and Engineering, Ritsumeikan University, 1-1-1 Noji Higashi, Kusatsu, Japan. gr0120pr@ed., wangzk@fc., hirai@se.ritsumei.ac.jp

[2]Yohan Noh and Thrishantha Nanayakkara are with the Department of Informatics, King's College London, London, UK. yohan.noh@, thrish.antha@kcl.ac.uk

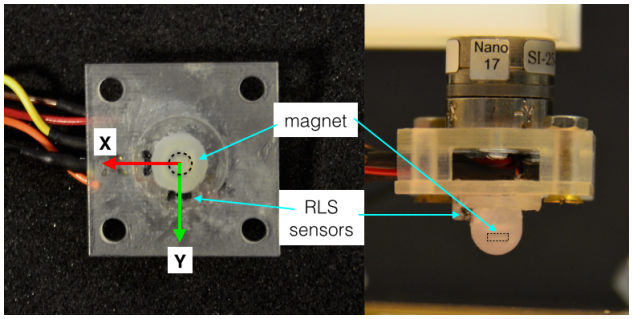

Fig. 1. Constructed soft force sensor. The magnet is inside the soft layer. RLS are aligned in the x, y, z directions measuring the magnetic flux induced by the magnet.

There are number of force sensor technologies available. A state of the art survey on the different technologies for force and torque measurement are presented in [1] emphasizing the use of these in MIS. Strain gauge based sensors are the common type. Yamamoto [2] measured force and torque by strain gauge based sensors. However, these sensors' usage is constrained by size, geometry, cost and inability to withstand above mentioned heat and pressure.

Optical technology based sensors are being made small enough to be fixed into the endoscope. Puangmail [3] made a rolling indent that measured stiffness using optical proximity sensors and Faragasso [4] introduces a stiffness probe that could be attached to an endoscope. Both were used to discriminate different tissue stiffness in MIS. One disadvantage of these sensors was these could not to be used together with magnetic resonance imaging (MRI) scanners due to the electrical components inside the sensor being damaged. To overcome this, Puangmail [5] developed a MRI compatible force sensor for cardiac surgeries.

Not only MIS, teleoperation would also greatly benefit from soft force sensor technologies. Rosen [6] developed a teleoperated endoscopic grasper that measures forces and controlled using force inputs. Other types of force sensors such as micro electromechanical force sensors were also introduced [7], [11]. The size of these sensors is an advantage for biomedical applications if the measurements are in vivo. But if the measurements are outside the body, compound sensors such as biomimetic fingertips [8] can be utilized. These too could measure force and vibration modalities.

This paper introduces a 3d force sensor (Fig. 1) capable of measuring either forces or displacements. The sensor has a soft cylindrical beam element that compresses and bends when a force is applied to the free end of the beam. A niobium permanent magnet is embedded inside the

978-1-4244-9270-1/15/$31.00 ©2015 IEEE

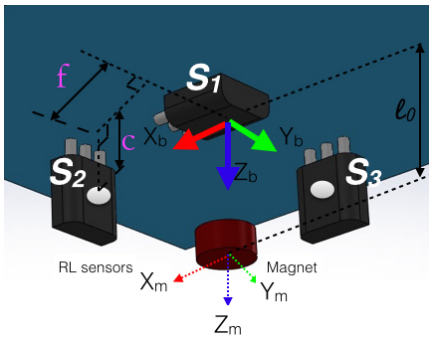

(a)

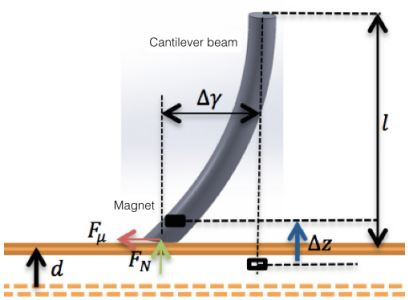

(b)

Fig. 2. (a) Coordinate system used for the calculation of the change in magnetic flux near RLS. The RLS sensors are perpendicular to each other, resulting in x,y,z orthogonal coordinates.X_b,Y_b,Z_b are base coordinates and X_m,Y_m,Z_m are magnet coordinates, (b) The sensor element is assumed as a cylindrical cantilever beam element influenced by a horizontal and vertical load F_μ,F_N. The end of the cylinder has a displacement of x,y,z while magnet has a displacement of $\Delta x,\Delta y$ and Δz.

cylinder. Three ratiometric linear sensors (RLS) or hall effect sensors which are perpendicular to each other surrounds the cylindrical beam. When the cylinder bends, the magnet is displaced from the original location. Then the magnetic flux near the RLS also changes. By analysing these changes of the magnetic flux, force and displacement can be calculated referring a lookup table. The paper introduces the sensor, its working principle and the calibration. The sensing principle (sensing magnetic flux) was an adaptation of [9].

II. CHARACTERIZATION OF THE SENSOR

The tactile sensor (Fig.1) was made of soft material (Smooth-on Dragon Skin 30) embedding a Niobium cylindrical magnet of diameter 2 mm. The cylindrical cantilever with a diameter of $D=8$ mm, and a total length of $L=9$ mm (length of cylindrical cantileve $L_{cyl}=5$ mm) had a hemispherical end so that an applied force goes through the centre of the cylinder every time. The magnet was placed at the centre of the hemisphere. Outside this soft layer were three Honeywell SS495A ratiometric linear sensors (RLS) or hall effect sensors perpendicular to each other. Sensors on the x,y directions were placed at a distance of 5 mm from the axis of the cantilever. The components and materials cost of the sensor were totalled to less than $10. When an external force was applied to the soft silicon hemisphere, the material deformed, displacing the magnet inside and causing the magnetic flux to change near the RLS. The magnetic field of a permanent magnet can be calculated from the vector potential: $\mathbf{B}=\nabla\times\mathbf{A}$. Here $\mathbf{A}$ is magnetic potential. The magnetic potential at point $\mathbf{X}$ is given by the following surface integral [10]:

$$\mathbf{A}=\frac{\mu_0}{4\pi}\oint\frac{\mathbf{M}(\mathbf{X}')\times\hat{n'}}{|\mathbf{X}-\mathbf{X}'|}da' \tag{1}$$

where $\mathbf{M}$ is the volume magnetization of the magnet, $\hat{n'}$ is the unit vector normal to the surface at a point $\mathbf{X}'$, and μ_0 is the permeability of air. The integral is performed over the entire surface of the magnet. For a cylindrical magnet the above equation can be solved by converting the magnet's (X_m,Y_m,Z_m) orthogonal coordinates to cylindrical coordinates. The cylindrical coordinate (ϕ,ρ,Z) represents an arbitrary point (Fig. 2(a)) in space outside the magnet. It can be noted that the magnetic flux is symmetric along direction ϕ as cylinder has a symmetry. Then equation (1) can be reduced to represent a magnetic flux distribution $\phi_m$on a plane having an angle of ϕ with ρ,Z axis:

$$\phi_m(\rho,Z)=\frac{\mu_0}{4\pi}M\iiint\frac{(z-Z)R\,\mathrm{d}R\mathrm{d}z\mathrm{d}\alpha}{[\rho^2-2R\rho\cos\alpha+R^2+(z-Z)^2]^{3/2}} \tag{2}$$

solving this equation yields the following:

$$\begin{aligned}B_z=&-\frac{\mu_0}{4\pi}M\int_0^{2\pi}\int_0^{a}[\frac{R(L/2-z)}{[R^2+(L/2-z)^2+\rho^2-2R\rho\cos\alpha]^{3/2}}\\&+\frac{R(L/2+z)}{[R^2+(L/2+z)^2+\rho^2-2R\rho\cos\alpha]^{3/2}}]\mathrm{d}R\mathrm{d}\alpha\\B_\rho=&-\frac{\mu_0}{4\pi}M\int_0^{2\pi}\int_0^{a}[-\frac{R(2\rho-2R\cos\alpha)}{2[R^2+(L/2-z)^2+\rho^2+2R\rho\cos\alpha]^{3/2}}\\&+\frac{R(2\rho-2R\cos\alpha)}{2[R^2+(L/2+z)^2+\rho^2-2R\rho\cos\alpha]^{3/2}}]\mathrm{d}R\mathrm{d}\alpha\end{aligned} \tag{3}$$

finally, the magnitude of the magnetic flux given in units of weber (Wb) at a given point can be calculated as:

$$B_{tot}=\sqrt{B_z^2+B_\rho^2} \tag{4}$$

From calibration tests, we found that RLS has a conversion factor of 3.9578×10^6 volts per weber. Therefore, by measuring the sensor's output voltage we could measure the magnetic flux induced by the magnet at the location of the sensor.

1) Force Calculation: Next, assume at the end of the cylinder, two forces F_n,F_μ are applied. These forces are perpendicular to each other. Due to the lateral force F_μ, the cylinder bent $\Delta\gamma$ at the end. This bending force can be assumed equal to the friction between the soft cylinder and the contact surface when there is a relative motion. The force F_N which is normal to the contact surface is compressing the soft cylindrical beam for a depth of d. We assume that the soft cylinder behaves like a cantilever elastic beam (Fig.

2(b)). We then write the compression and bending equations as follows:

$$F_N = \frac{EA}{L}d \tag{5}$$

The lateral force F_μ is calculated from the bending formula as:

$$F_\mu = -3EI\frac{\Delta\gamma}{l^3} \tag{6}$$

where A, E, L, I are cross sectional area of beam, Youngs modulus of soft material, natural length of beam and moment of inertia of the cross section of the cantilever beam. Youngs modulus is selected as 1.0 MPa. Cross sectional area of the cantilever beam is calculated as:

$$A = \pi.[(\frac{D}{2})^2 - (\frac{D}{2}+d)^2] \tag{7}$$

here D is the diameter of the cantilever beam and d is the deformation of the contact point in z direction.

2) Displacement Calculation: Due to the normal and frictional force F_N, F_μ, the end of the soft cylinder moves x, y, z from the initial position causing the magnet to move $\Delta x, \Delta y, \Delta z$. Then from geometric relations:

$$\Delta\gamma = \sqrt{\Delta x^2 + \Delta y^2} \tag{8}$$

$$\Delta z = l + d - e \tag{9}$$

$$\Delta x = [\frac{(L-d)-(\Delta z+e+d)}{(L-d)}]x \tag{10}$$

$$\Delta y = [\frac{(L-d)-(\Delta z+e+d)}{(L-d)}]y \tag{11}$$

where e is the unstressed distance from the end of the cantilever beam to the centre of the magnet. Then, the coordinates of the RLS sensors ($S_1, S_2$and S_3) can be written from the magnet coordinate system (ϕ, ρ, Z) as:

$$S_1 : \quad (\phi_1, l, \Delta\gamma)$$

$$S_2 : \quad (\phi_2, l-c, \sqrt{\Delta y^2 + (f+\Delta x)^2})$$

$$S_3 : \quad (\phi_3, l-c, \sqrt{\Delta x^2 + (f+\Delta y)^2})$$

as magnet has a symmetry around its z axis, the magnetic flux around axis at a distance of (ρ, Z) is same for a given ϕ. Therefore ϕ_1, ϕ_2, ϕ_3 are ignored in these calculations.

III. EXPERIMENTS AND RESULTS

A lookup table of the sensor had to be constructed before using the sensor. The relationship between applied normal force F_N and contact depth d and the relationship between normal force F_N and the RLS signal of the z axis sensor V_{S_z} was evaluated. For this paper only the z axis deformations were presented. It should be noted that the same steps can be used to calculate x, y directional forces (F_μ) and displacements.

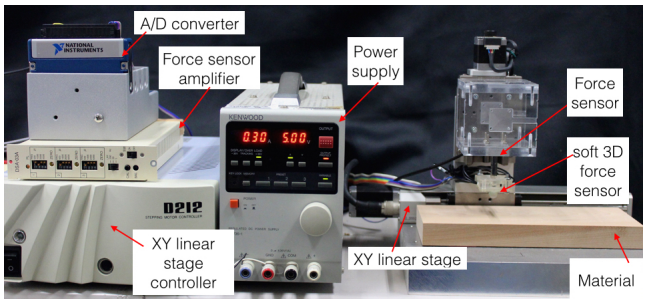

Fig. 3. Experimental setup

A. Hardware setup

The experimental setup is shown in Fig.3. The system consists of a soft tactile sensor rigidly fixed to the vertical linear stage of the XY table (Suruga Seiki KXL06100-C2-F) via a Tech Gihan (USL 06-H5-50N-C) force sensor. The vertically moveable linear stage is fixed to a horizontal linear stage. Both stages allow the tactile sensor to move in the x and z directions. The linear stages has a step size of 4 μm. The force sensor is capable of measuring the forces in three dimensions. The force sensor has an amplifier of its own and the processed signal is sent to a National Instruments NI9205 analog to digital converter.

The linear stages, and the AD converters are connected to a computer and controlled through LabView software. The Data retrieval and the linear stage motion are synchronized by the software. The sampling rate of the AD converter was 1000 Hz.

B. Experiments and Simulations

For constructing the look up table, normal force F_N was applied by pushing the soft tactile sensor onto a hard surface for a depth d. The sensor was stationary in the horizontal direction $(F_\mu = 0)$. The force was measured using the force sensor. The displacement was measured using the encoders in the linear stage. The voltage output of the three RLS $V_{S_x}, V_{S_y}, V_{S_z}$ were recorded for each step of the normal force F_N and the deformation d. The depth of the contact was changed with steps of 4 μm. The average of the voltages for increase in depth and decrease in depth were calculated and saved in a table. The experiment was conducted five times and the average value for each step was taken in the construction of figure 4.

Figure 4, shows the relationship between the contact depth d and the normal force F_N. Furthermore by using equation 5, normal force was calculated mathematically. It can be noted that the simulated value and the actual values are non-linear but up to depth $d = 1.5$ mm (from Fig.4) or normal force $F_N =$ 1.5N (from Fig.6), the error between the actual and the simulated value were under 5% which is acceptable for a initial system such as this.

Furthermore, figure 5 shows the relationship between the normal force F_N and the voltage of the sensor 1 V_{S_z}. The figure shows that the maximum histerisis of the sensor is within 10% and the simulated values and the actuated values

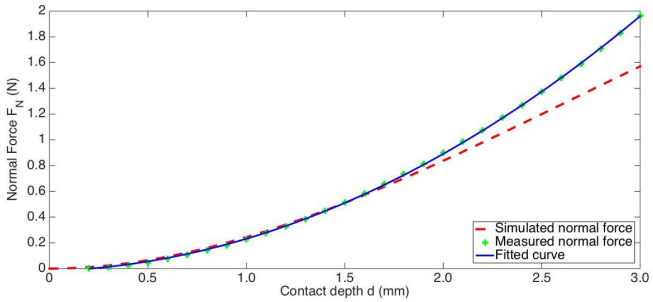

Fig. 4. Normal force F_N vs. contact depth d

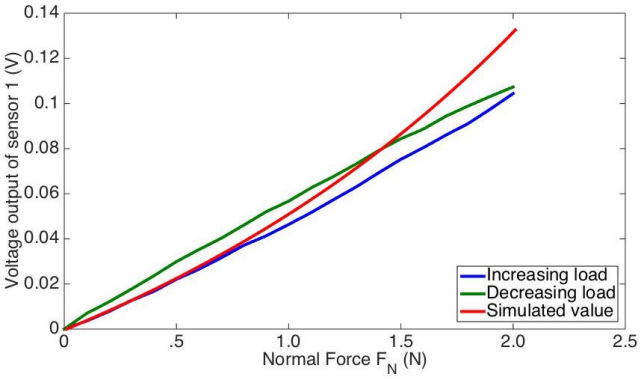

Fig. 5. Normal force F_N vs. z sensor voltage

till $F_N = 1.5\,\mathrm{N}$ are within 5%. range. Figure 6 is representing the x, y sensor outputs V_{S_x}, V_{S_y} for normal force. It shows that x, y, z directional force measurement are coupled with each other. If $F_\mu \neq 0$, the voltages of x, y directional sensors will behave according to the direction of the force.

IV. CONCLUSIONS

This paper introduces a novel soft sensor for biomedical applications. It operates by measuring the deformation of a soft cylinder and calculating the compressive and bending forces applied at the end of the cylinder. The 3D deformations are calculated by measuring the changes in the magnetic field when a magnet is displaced from its initial position. The magnetic field is measured by three orthogonal RLS and the special displacement in calculated from those measurements. The analysis shows that the force calculated from the three sensor voltages obtained, can be fitted to a third order polynomial. Though the force calculations require computationally intensive steps, the cheap construction of the sensor provides advantage to many existing force sensors. The calculated and measured force values have some deviation after 1.5 mm contact depth or 1.5 N normal force and it could be explained from the assumption taken at the beginning of the calculations as the sensing element is a cylinder while actually it is a cylinder with a hemisphere at the end. Furthermore, the calculation of the magnetic field neglects the orientation of the niobium magnets. It is believed the magnet's orientation is a significant variable and future research need to account that as a variable. The sensor's force calculations in x and y directions are coupled

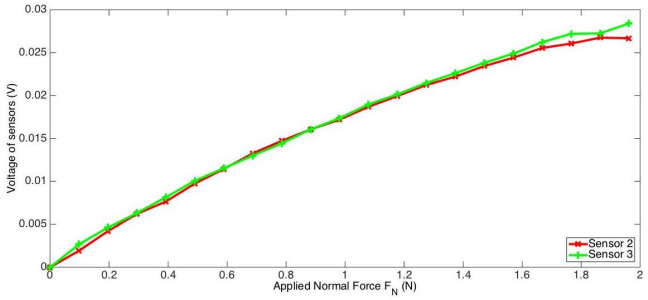

Fig. 6. Normal force F_N vs. x, y directional sensors voltage (sensor 2 and sensor 3)

with the z directional displacement. Furthermore, additional experiments have to be carried out to investigate the effects of properties in the soft overlay affecting the calculated force values. It is believed that the system can be miniaturized further and it needs to be investigated in future.

REFERENCES

[1] P. Puangmali, K. Althoefer, L.D. Seneviratne, D. Murphy, and P. Dasgupta, State-of-the-art in force and tactile sensing for minimally invasive surgery IEEE sensors Journal, vol. 8, no. 4, pp. 371-381, 2008.

[2] T. Yamamoto, B. Vgvlgyi, K. Balaji, L.L. Whitcomb, and A.M. Okamura, Tissue property estimation and graphicldisplay for teleoperated robot-assisted surgery. IEEE Inernational Conferance on Robotics and Automation, pp.4239-4245, 2009.

[3] P. Puangmali, H. Liu, L.D. Seneviratne, P. Dasgupta, and K. Althoefer, Miniature 3-axis distal force sensor for minimally invasive surgical palpation IEEE/ASME Transactions on Mechatronics, vol. 17, no. 4, pp.646-656, 2012.

[4] A. Faragasso, A.Stilli, J. Bimbo, Y. Noh, H. Liu, T. Nanayakkara, P. Dasgupta, H.A Wurdemann, and K. Althoefer, Endoscopic add-on stiffness probe for real-time soft surface characterisation in MIS IEEE Engineering in Medicine and Biology Society Conferenace, pp.6517-6520, 2014.

[5] P. Puangmali, A. Ataollahi, T. Schaeffter, R. Razavi, L.D. Seneviratne, and K. Althoefer, MRI-compatible intensity-modulated force sensorfor cardiac cathetrization procedures. IEEE Transactions on Biomedical Engineering, vol.58, pp.721-726, 2011.

[6] J. Rosen, B. Hannaford, M.P. MacFarlane, and N. Sinanan, Force controlled and teleoperated endoscopic grasper for minimally invasive surgery-experimental performance evaluation, IEEE Transactions on Biomedical Engineering, vol.46, pp.1212-1221, 1999.

[7] F. Tendick, S. S. Sastry, R. S. Fearing, and M. Cohn, Applications of micromechatronics in minimally invasive surgery, IEEE/ASME Trans. Mechatron., vol. 3, pp. 34?42, 1998.

[8] D. S. Chathuranga, V. A. Ho and S. Hirai, Investigation of a biomimetic fingertip's ability to discriminate fabrics based on surface textures, IEEE/ASME International Conference on Advance Intelligent Mechatronics, pp.1667-1674 , 2013.

[9] S. Takenawa, A soft three-axis tactile sensor based on electromagnetic induction, IEEE International Conference on Mechatronics, pp.1-6 , 2009.

[10] J.D. Jackson, Classical Electrodynamics, 3rd edition, Wiley, 1998.

[11] P. Peng, A.S. Sezen, R. Rajamani, and G. Erdman, Novel MEMS stifness sensor for in-vivo tissue characterization measurement, IEEE Engineering in Medicine and Biology Society, pp.6640-6643, 2009.